



## MECHANICAL AND EROSIWE WEAR BEHAVIOUR OF CLAY FILLED POLYAMIDE66/ POLYPROPYLENE NANO COMPOSITES

\*Suresha B <sup>1</sup> and Mohammed Ismail <sup>2</sup>

<sup>1</sup> Department of Mechanical Engineering, The National Institute of Engineering, Mysore, Karnataka-570008, India

<sup>2</sup> Department of Industrial & Production Engineering, The National Institute of Engineering, Mysore, Karnataka -570 008, India.

### ABSTRACT

The current work presents an attempt to study the mechanical and erosive wear behaviour of clay filled polyamide66/polypropylene (PA66/PP) nanocomposites. PA66/PP blend was used as a reference material. The erosion wear volume loss of the composites have been evaluated for different impingement angles (30–90<sup>0</sup>) and at a constant impingement velocity of 29 m/s. Mechanical properties such as tensile strength, ultimate elongation at fracture and hardness seems to be controlling the erosion wear volume loss of PA66/PP blend and clay filled PA66/PP nanocomposites. Clay filled PA66/PP nanocomposite showed semi-ductile erosion behaviour with peak erosion weight loss at 45<sup>0</sup> impingement. However, the unfilled PA66/PP blend showed the maximum erosion wear volume loss at 30<sup>0</sup> impingement. It was observed that the nanosized clay filler helps in improving the erosive wear resistance of PA66/PP blend. Worn surface features of the samples were examined using scanning electron microscope to understand the involved wear mechanisms.

**Keywords:** *Clay Filled PA66/PP Nanocomposites, Mechanical Behaviour, Erosive Wear and Worn Surface Morphology.*

### 1. Introduction

Composite materials offer exciting advantages over traditional monolithic materials. Modern advanced composites are a success story from the view point of their widespread applications, ranging from tennis rackets to advanced space vehicles. Aggressive research has been carried out worldwide to explore the new composites with improved functional properties.

Clay filled polymer nanocomposites have been the subject of many recent papers due to their excellent properties and potential industrial applications [1-4]. In principle, small amount of nanosized fillers, in the range of 3 to 5% by wt. can provide comparable properties as 30 to 50% by wt. of micro-sized fillers do in conventional composites. The performance of polymer nanocomposites largely depends upon the spatial distribution arrangement of intercalating poly chains and interfacial interaction between the silicate layers and the polymers [5-6]. Since, natural montmorillonite (MMT) is hydrophilic; there is no good affinity to the polymer, which resulted in intercalated or partially exfoliated structure [7-9]. Organic modifications, levels the surface energy of the clay layers by providing such hydrophobic functional groups and impress the interfacial characteristics, required to disperse the clay into the polymer matrix [10].

The erosion of materials caused by impact of hard particles is one of several forms of material degradation generally classified as wear. Solid particle erosion is the progressive loss of original material from a solid surface due to mechanical interaction between the surface and impinging particles. Solid particle erosion is a serious problem in gas turbines, rocket nozzles, cyclone separators, valves, pumps and boiler tubes. Polymer composite materials are finding increased application under such conditions in which they may be subjected to solid particle erosion [11].

Damage caused by erosion has been reported in several industries for a wide range of situations. Examples have been cited for transportation of airborne solids through pipes by Bitter [12], boiler tubes exposed to fly ash by Raask [13] and gas turbine blades by Hibbert and Roy [14].

Various applications of polymers and their composites in erosive wear situations were reported in the literature [15-22]. But solid particle erosion of polymers and their composites has not been investigated to the same extent as for metals or ceramics. However, a number of researchers, Kulkarni and Kishore [16], Aglan et al. [17], Barkoula and Karger-Kocsis [18], Harsha et al. [19], and Tewari et al. [20, 21] have

\*Corresponding Author - E- mail: sureshab2004@yahoo.co.in

evaluated the resistance of various types of polymers and their composites to solid particle erosion. The effect of Solid particle than that of neat polymer was reported by Hager et al. [22]. The solid particle erosion behavior of polymer composites as a function of fiber content has been studied to a limited extent by Miyazaki and Takeda [23]. Tilly and Sage [24]. They studied the various parameters such as the influence of velocity, impact angle, particle size and weight of impacted erodent on nylon, carbon fiber reinforced nylon, neat epoxy, polypropylene and glass fiber reinforced polypropylene. Erosive wear of the turbine blades is a complex phenomenon that depends on: (i) eroding particles, their size, shape, hardness and concentration (ii) substrates, chemistry, elastic properties, surface hardness and surface morphology and (iii) operating conditions, velocity and impingement angle [25]. The erodent shape is an important property, but its effect is difficult to quantify for natural particles. For impact of spherical particles on ductile materials, Hutchings and Winter [26] assumed ploughing of material forming lips around the crater, which breaks up in subsequent impact. In another study, Winter and Hutchings [27] have shown that the angular particles remove the material by ploughing and micro cutting for lead and mild steel. Desale et al. [28] have shown that the surface morphology of substrate material has deep craters and higher value of average surface roughness for angular erodent particles compared with the blocky shape erodent. Suresha et al. [29, 30] have evaluated the tribological properties of unfilled and nanoclay filled polymer matrix composites.

Polypropylene exhibits many beneficial properties such as low density, relative high thermal stability, and resistance to chemical attack, easy processing and recyclability. The property that accounts for the popularity of polyamide is high crystalline melting point good resistance to hydrocarbons, high strength, and ease of processing and fabrication. Mixing two polymers usually leads to immiscible blends, characterized by a coarse, metastable morphology, and poor adhesion between the phases. For improved performance the immiscible blends usually need compatibilization. As compatibility increases, the average domain size of the dispersed phase will decrease and the ability to transfer stresses from one domain to another without separation will increase. This trend can be thought of one in which the interfacial adhesion of the two materials is being increased. Hence in this research work, the influences of nanoclay on the mechanical and erosive wear behaviour of PA66/PP composites with maleic anhydride polypropylene as compatibilizer was investigated. The effect of particulate filled polymer composites on erosion

characteristics has also not been widely reported in the literature.

The objective of the present work is to study the solid particle erosion of nanoclay filled PA66/PP blend composites under various experimental conditions.

## 2. Experimental Details

### 2.1 Materials used

Polymer alloy of polyamide66 and polypropylene and particulate nanoclay (NC) filled PA66/PP composites were prepared for this study with compatibilizer. The polymer alloy produced consists of 50 % by wt. of each of the constituent. Maleic anhydride polypropylene (MAGPP) as compatibilizing agent was used in this study. The amount of compatibilizer added was 1 wt.% based on previous literature and this compatibilizer proportion was high enough for interaction with PA66/PP interface.

### 2.2 Compounding

Before compounding, the polymer granules and fillers were dried at 80°C for 10 h in an air circulated oven and then dry mixed with polyamide66 and other additives. Composition shown in below table was mixed and extruded in a co-rotating twin extruder. The length to diameter (L/D) ratio of the screw is 40:1. Mixing speed of 60 rpm was maintained for all the compositions. The extrudates from the die were quenched in a tank at 20-30 °C and then palletized. For the melt blending the temperature profile of the extrusion were Zone 1(205 °C) Zone 2(235 °C) Zone 1(245 °C) Zone 1(255 °C) and at die (265 °C).The extrudates of the composition was palletized in palletizing machine. The rpm of the pelletizer was maintained between the ranges of 70 rpm.

### 2.3 Injection molding

The granules of the extrudates were pre dried in air circulated oven at 80°C for 10 h and injection molded in a microprocessor based injection moulding machine fitted with a master mould containing the cavity for tensile, flexural and impact specimens. After its ejection from the mould, specimens were cooled in ice-water. Processing parameters are Zone 1(200 °C) Zone 2(235 °C) Zone 1(260 °C).

### 2.4 X-ray diffraction

The interlayer distance of nanoclay in the nanocomposites was studied by wide angle X-ray diffraction. Both for the nanoclay and the nanocomposites, XRD was recorded using X-ray diffractometer (RIGHKU-Make), Copper Ka target is

used. The basal spacing reflection of samples was calculated from Bragg's equation by monitoring the diffraction angle  $2\theta$  from  $2 - 10^\circ$  at scanning rate of  $0.5^\circ/\text{min}$ .

### 2.5 Mechanical characterization

Hardness (shore-D) measurement is done using a Shore hardness tester. The tensile test is performed on flat dog-bone shaped composite specimens as per ASTM D-638 test standards using a universal testing machine Instron 1195.

### 2.6 Erosion test method

Fig. 1 shows the schematic diagram of erosion test rig conforming to ASTM G-76. The set up is capable of creating reproducible erosive situations for assessing erosion wear resistance of the prepared composite samples. It consists of an air compressor, an air particle mixing chamber and an accelerating chamber. Dry compressed air is mixed with the particles which are fed at constant rate from a sand flow control knob through the nozzle tube and then accelerated by passing the mixture through a convergent brass nozzle of 3 mm internal diameter. These particles impact the specimen which can be held at various angles with respect to the direction of erodent flow using a swivel and an adjustable sample clip.

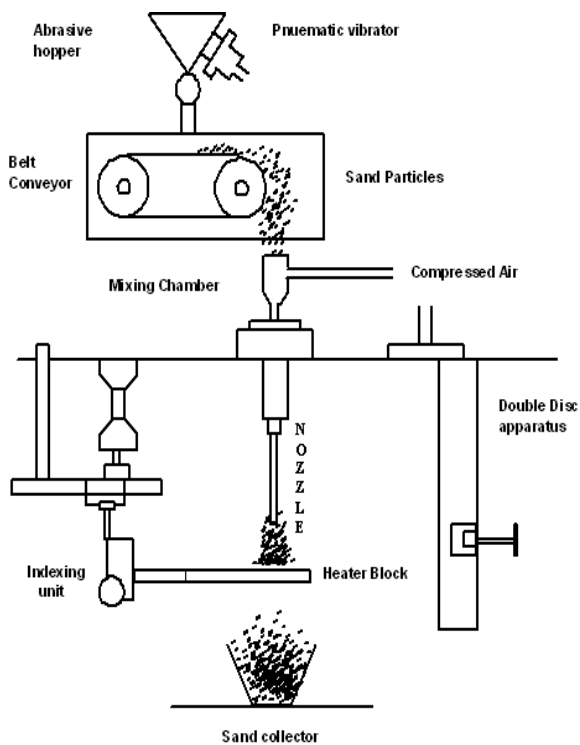


Fig. 1 Schematic Diagram of the Erosion Test Rig

The velocity of the eroding particles is measured using double disc method. In the present study, dry silica sand (angular) of particle size ranging between 200 to 250  $\mu\text{m}$  used as erodent. Each sample is cleaned in acetone, dried and weighed to an accuracy of  $\pm 0.1$  mg using a precision electronic balance. It is then eroded in the test rig for 1min and weighed again to determine the weight loss. The erosion volume loss was then calculated by measuring the density using Archimede's principle.

The process is repeated till the erosion rate attains a constant value called steady-state erosion rate. The conditions under which the erosion tests were carried out are listed in Table 1. Square samples of size 50 mm  $\times$  50 mm  $\times$  2.2 mm were cut from the slabs for erosion tests. A standard test procedure (ASTM G-76) was employed in the present study. The samples were cleaned in acetone, dried and weighed to an accuracy of  $1 \times 10^{-5}$  g using an electronic balance (Mettler Toledo), eroded in the test rig for 1 min and then weighed again to determine erosion weight loss.

Table 1: Test Parameters Selected for Erosion Test

Erodent	Silica sand
Erodent size ( $\mu\text{m}$ )	200–250
Erodent shape	Irregular, slightly rounded
Impingement angle ( $^\circ$ )	15, 30, 45, 60 and 90
Impact velocity (m/s)	$28 \pm 2$
Erodent feed rate (g/min)	$4.7 \pm 0.3$
Nozzle to sample distance and nozzle diameter (mm)	10 and 4

## 3. Results and Discussion

### 3.1 X-ray diffraction

Fig. 2 shows the XRD pattern in the range of  $2\theta = 2 - 10^\circ$  for nanoclay and PA66/PP nanocomposites. The XRD pattern of the nanoclay shows a broad intense peak at around  $2\theta = 4.2^\circ$  corresponding a basal spacing 21.03 $\text{\AA}$  (By using Bragg's law  $2d \sin \theta = n\lambda$ , where  $\lambda$  is the X-ray wave length (1.54  $\text{\AA}$ ),  $2\theta = 4.2^\circ$ ).

The XRD pattern of PA66/PP, nanoclay filled PA66/PP, graphite filled PA66/PP composites do not show a characteristics basal reflection of the nanoclay. However they show shoulder at  $2\theta = 2^\circ$ . This is a clear indication that portion of nanoclay is only intercalated. Wahit et al. [31], Chow et al. [32] have reported a similar observation in the case of

polyamide/polypropylene nanocomposites. The absence of the characteristic clay  $d_{001}$  peak indicates the exfoliation of the clay platelets in the PA66/PP matrix.

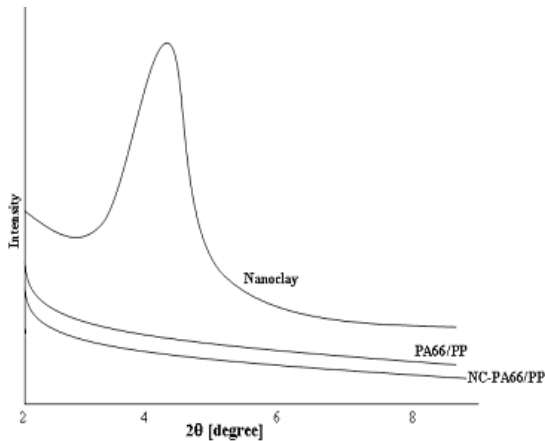


Fig. 2 XRD Spectra for the Clay and PA66/PP Nanocomposites

3.2 Physico-mechanical properties

Table 2 gives the hardness values for different compositions. It is seen that with inclusion of clay in the composite, its hardness value improves although the filler loading is marginal. The density and mechanical properties such as tensile strength and strain of unfilled PA66/PP and clay filled PA66/PP composites are listed in Table 2. From Table 2, it can be seen that nanoclay greatly decreased the tensile strength and strain of PA66/PP blend, which can be attributed to poor interfacial adhesion between clay and PA66/PP blend. Also, it clearly indicates that inclusion of nanoclay deteriorates the load bearing capacity. The density of PA66/PP blend is  $0.9072 \text{ g/cm}^3$  and increased to  $1.0287 \text{ g/cm}^3$  for clay filled PA66/PP nanocomposite. This is due to the high density of clay in PA66/PP blend.

Table 2: Density and Mechanical Properties of Clay-filled PA66/PP Composites

Samples	PA66/PP	NC-PA66/PP (2.5 wt.%)
Tensile strength (MPa)	30.65	22.20
Strain (%)	0.13	0.08
Hardness (Shore-D)	64	71
Density ( $\text{g/cm}^3$ )	0.9072	1.0282

3.3 Erosion behaviour

Fig. 3 is a plot showing the erosion wear volume loss of unfilled and clay filled PA66/PP

nanocomposites tested as a function of the angle of impingement and at a constant impinging velocity of 29 m/s. It is quite evident from Fig. 2 that the wear volume loss initially increases with increase in the impingement angle, attains a peak value at  $45^\circ$  and then starts decreasing as the impact angle moves towards  $90^\circ$  for clay filled PA66/PP. These trends are exhibited for 2.5 and 3 wt.% filler loading and wear volume loss decreases with increased filler loading. However, erosion volume loss is strongly affected by the variation of impingement angle of the particles. The filled composites showed lower values than that of unfilled composites. Further, for unfilled PA66/PP blend, the wear volume loss initially it is very high and decreases with increase in impingement angle. From Fig. 3 it is clear that strong dependency of the erosive wear exists as a function of the constituents of the composites.

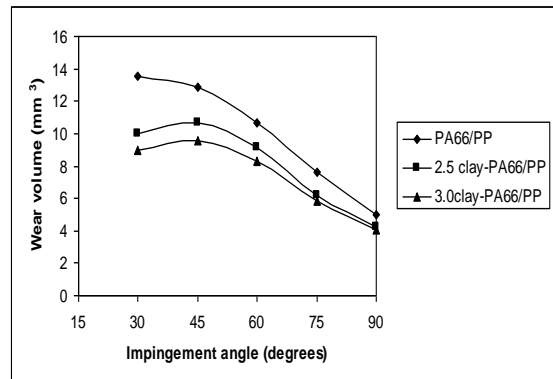


Fig. 3 Variation of Wear Volume loss of PA66/PP and Clay filled PA66/PP Nanocomposites.

This is because of the fact that when a composite surface is eroded by solid particles, the material lost is composed of particulate clay and polymer blend. The increase of the solid particle erosion resistance of the clay filled PA66/PP composite is increased as the filler weight fraction. To the contrary, the tensile strength of the composite decreased with nanoclay filler addition in the PA66/PP blend.

It is evident from the plot that the erosion wear volume decreases with the impact angles and attains a peak value at  $30^\circ$  for PA66/PP blend.. It is also found that at impact velocity of 29 m/s, minimum and maximum erosion wear volume are at  $90^\circ$  and  $30^\circ$  for PA66/PP. However, for NC-PA66/PP composites, the minimum and maximum erosion wear volume is at  $90^\circ$  and  $45^\circ$ . In general maximum erosion rate for ductile material remains in the range  $15^\circ - 30^\circ$  and minimum

erosion rate at 90°. While for brittle material the behavior is opposite. It is available in the literature that, there are no fixed trends available which correlates ductility or brittleness of materials with maximum or minimum erosion rate. From the erosion data, it is clear that the effect of increasing nanoclay content (0 to 3 wt.%) has influence on mechanical and erosion behaviour, because some properties of nanoclay layers such as high modulus are shared with PA66/PP blend. By going to higher levels of nanoclay does not show further improvement, may be due to difficulties in getting better dispersions and exfoliation of clay in the PA66/PP blend. It is found that some polymers erode in a ductile manner; some show evidence of both ductile and brittle characteristics [22, 34].

### 3.4 Worn surface morphology

Material microstructure plays an important role in determining the active wear mechanism in polymer matrix composites. Scanning electron microscopy (SEM) studies seem to support the difference in wear behaviour observed under different experimental conditions.

Erosion wear behaviour can be classified as ductile and brittle erosion although this grouping is not definitive. Thermoplastic matrix composites usually show ductile erosion while the thermosetting ones erode in a brittle fashion. SEM of neat PA66/PP blend and the clay filled PA66/PP nanocomposite eroded with 200-250 µm silica sand particles impacting at 30° and 45° and at an impingement velocity of 29 m/s are as shown in Figs. 4 and 5 respectively. The material removal is caused by the microcutting and microploughing process in which the material reveals a large plastic deformation at the impacted location (Fig. 4).

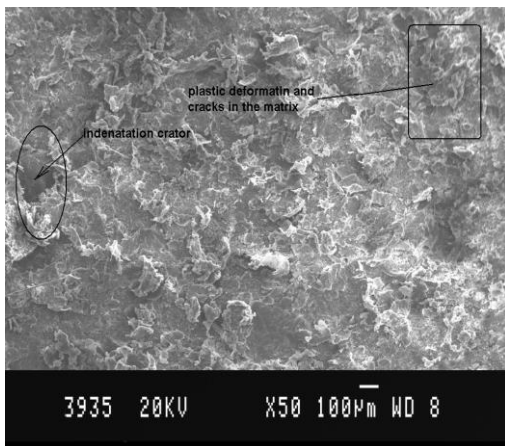


**Fig. 4 SEM of Single Impacted Surface for Velocity 29 m/s and Impingement Angle of 30° for PA66/PP Blend**

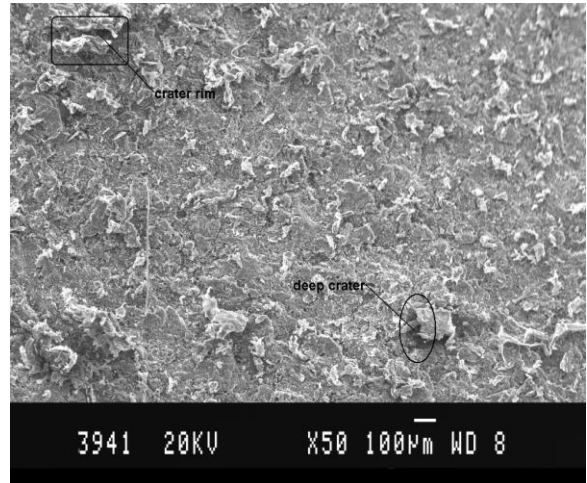


**Fig. 5 SEM of Single Impacted Surface for Velocity of 29 m/s and Impingement Angle 45° for Clay Filled PA66/PP.**

It can be seen that the plastic strain is very high at an impingement angle of 30° for the target material. The plastic deformation at 90° impact angle is greater than the situation at 30°, but the erosion volume loss at 90° impact angle is less than the situation at 30°. The eroded surface showed the formation of larger crater volume (Fig. 4). Further, it can be seen from the figure that the neat polymer blend surface exhibits irregular-shaped distributed debris due to the actions of erodent involving plastic deformation and more cracks owing to lower hardness. The worn surface of neat polymer blend showed severe matrix damage and more cracks throughout the sample surface.

The wear pattern for silica sand particles with clay filled PA66/PP composite as the target material is shown in Fig. 5. From the results of shore D hardness tests, it is clear that the hardness of neat PA66/PP blend is less than that of clay filled PA66/PP composites. The harder the material, lesser the crater volume that is removed and hence the erosion volume loss is less. It is clear from Fig. 3 that 2.5 and 3 wt% filled PA66/PP composites show lower erosion volume loss. This may be due to the restriction of debonding between matrix and filler, which is seen in Fig. 4. The hard surface has resulted in shallow penetration and thus causes less erosion. From SEM observations of the eroded surface, it appears that composites under consideration exhibit several stages of the erosion and material removal process. It can be seen that the material removal in this region is being removed by deformation showing deep craters due to normal impact of particles. Deep craters are dominant and impacting particles forms rims around the crater, which may get flattened and

fractured by subsequent impact of particles. High deformation of the surface with deep indentation craters and local microcracks are seen (Fig. 5) where the target material hardness is significantly lower compared to that of the erodent. The highest surface roughness values have been observed in this region. This may be attributed to the lower hardness of the target materials, which forms deep craters due to impact of hard particles. The variation of the wear volume loss in this region can be attributed to the material properties other than hardness of target and erodent.

#### 4. Conclusions

Based on the solid particle erosion studies of unfilled and clay filled PA66/PP nanocomposites, the following conclusions were drawn.

- i. The XRD results indicate that the nanoclay is more uniformly dispersed in the PA66/PP blend.
- ii. Impingement angle and the material properties such as matrix and particulate filler have strong influence on the erosive wear performance.
- iii. The angle of impact is the most important parameter during erosion. The angle of impact greatly affects the erosion wear behavior of PA66/PP blend and clay filled PA66/PP nanocomposites.
- iv. The erosive wear behaviour strongly depends on impingement angle. Depending on the angle of impingement, the order of wear performance of unfilled PA66/PP and clay filled PA66/PP nanocomposites has changed significantly.
- v. The unfilled PA66/PP has shown peak erosion wear volume loss at 30° impingement angle. However, clay filled PA66/PP nanocomposite showed peak erosion wear volume loss at 45° impingement.
- vi. The effect of increasing nanoclay content (0 to 3 wt.%) has influence on mechanical and erosion behaviour, because some properties of nanoclay layers such as high modulus are shared with PA66/PP blend. By going to higher levels of nanoclay does not show further improvement, may be due to difficulties in getting better dispersions and exfoliation of clay in the PA66/PP blend.
- vii. Erosion processes in the clay filled PA66/PP composites were associated with the formation of deep craters and with microcrack propagation and intersection; this resulted in the formation of fragments of the debris which were then locally removed from the surface.

#### References

1. Andrew Mc Williams (2006), "Nanocomposites, Nanoparticles, Nanoclays and Nanotubes", BCC Research.
2. Li X and Ha C S (2003), "Nanostructure of EVA/Organoclay Nanocomposites: Effects of kinds of Organoclays and Grafting of Maleic Anhydride onto EVA", *Journal of Applied Polymer Science*, Vol. 87 (12), 1901-1909.
3. Fisher H (2003), "Polymer Nanocomposites: from Fundamental Research to Specific Applications", *Materials Sciences and Engineering: C*, Vol. 23 (6-8), 763-772.
4. Gupta R K and Bhattacharya S N (2008), "Polymer-Clay Nanocomposites: Current Trends and Challenges", *Industrial Chemical Engineering*, Vol. 50 (3), 242-267.
5. Giannelis E P (1996), "Polymer Layered Silicate Nanocomposites", *Advanced Materials*, Vol. 8 (1), 29-35.
6. Giannelis E P, Krishnamoorti R and Manias E (1999), "Polymer Silicate Nanocomposites: Model Systems for Combined Polymer and Polymer Brushes", *Advances in Polymer Science*, Vol. 138 (1), 107-147.
7. Song L, Hu Y, Wang S, Chen Z and Fan W (2002), "Study on the Solvothermal Preparation of Polyethylene/Organophilic Montmorillonite Nanocomposites", *Journal of Materials Chemistry*, Vol. 12 (2), 3152-3155.
8. Kurokawa Y, Yasuda H, Kashiwagi M and Oya A (1997), "Structure and Properties of a Montmorillonite/ Polypropylene Nanocomposite", *Journal of Materials Science Letters*, Vol. 16 (1), 1670-1672.
9. Theng B K G (2005), *Formation and Properties of Clay-Polymer Complexes*, Elsevier, Amsterdam.
10. Krishnamoorti R, Vaia R A and Giannelis E P (1996), "Structure and Dynamics of Polymer Layered Silicate Composites", *Chemical Materials*, Vol. 8(8), 1728-1734.
11. Hutchings I M (1992), "Tribology: Friction and Wear of Engineering Materials", Edward Arnold, UK.
12. Bitter J G A (1963), "A Study of Erosion Phenomena- Part II", *Wear*, Vol. 6 (3), 169-190.
13. Raask E (1969), "Tube Erosion by Ash Impaction", *Wear*, Vol. 13 (4-5), 301-315.
14. Aranda P and Ruiz-Hitzky E (1992), "Poly (ethylene oxide)-Silicate Intercalation Materials", *Chemical Materials*, Vol. 4 (6), 1395-1403.
15. Pool K V, Dharan C K H and Finnie I (1986), "Erosion Wear of Composite Materials", *Wear*, Vol. 107 (1), 1-12.
16. Kulkarni S M and Kishore (2001), "Influence of Matrix Modification on the Solid Particle Erosion of Glass/Epoxy Composites", *Polymer Composites*, Vol. 9 (3), 25-30.
17. Aglan H A and Chenock Junior T A (1993), "Erosion Damage Features of Polyimide Thermoset Composites", *SAMPEQ*, 41-47.

18. Barkoula N M and Karger-Kocsis J (2002), "Effect of Fiber Content and Relative Fiber Orientation on the Solid Particle Erosion of GF/PP Composite", *Wear*, Vol. 252 (1-2), 80–87.
19. Tewari U S, Harsha A P, Hager A M and Friedrich K (2002), "Solid Particle Erosion of Unidirectional Carbon Fiber Reinforced Polyetheretherketone Composite", *Wear*, Vol. 252(11-12), 992–1000.
20. Harsha A P, Tewari U S and Venkatraman B (2003), "Solid Particle Erosion Behaviour of Various Polyaryletherketone Composite", *Wear*, Vol. 254 (7-8), 693–712.
21. Tewari U S, Harsha A P, Hager A M and Friedrich K (2003), "Solid Particle Erosion of Carbon Fiber-and Glass Fiber-Epoxy Composites", *Composite Science & Technology*, Vol. 63(4), 549–557.
22. Hager A M, Friedrich K, Dzenis Y A and Paipetis S A (1995), "Study of Erosion Wear of Advanced Polymer Composites", Street K, Whistler B C (Eds.), *Proceedings of the ICCM-10, Canada*, Wood Head Publishing Ltd., Cambridge, 155–162.
23. Miyazaki N and Takeda T (1993), "Solid Particle Erosion of Fiber Reinforced Plastics", *Journal of Composite Materials*, Vol. 27(27), 21–31.
24. Tilly G P and Sage W (1970), "The Interaction of Particle and Material Behaviour in Erosion Process", *Wear*, Vol. 16(1), 447–465.
25. Mann B S (2000), "High- Energy Particle Impact Wear Resistance of Hard Coatings and their Application in HydroTurbines", *Wear*, Vol. 237(1), 140–146.
26. Hutchings I M and Winter R E (1974), "Particle Erosion of Ductile Metals: A Mechanics of Material Removal", *Wear*, Vol. 27 (1), 121–128.
27. Winter R E and Hutchings I M (1974), "Solid Particle Erosion Studies Using Single Angular Particles", *Wear*, Vol. 29(2), 181–194.
28. Desale G R, Gandhi B K and Jain S C (2006), "Effect of Eroding Properties on Erosion Wear of Ductile Type Materials", *Wear*, Vol. 261 (7-8), 914-921.
29. Ravi Kumar B N, Suresha B, Venkataramareddy M and Sampath kumara P (2010), "Friction and Dry Sliding Wear Characteristics of Particulate Filled Thermoplastic Nanocomposites", *Journal of Manufacturing Engineering*, Vol. 5(2), 80-86.
30. Suresha B (2008), "Influence of SiC Filler on Mechanical Properties of Glass Fabric Reinforced Polyester Composites", *Journal of Manufacturing Engineering*, Vol. 3(4), 256-260.
31. Wahit et. al, (2006), "Effect of Organoclay and Ethylene-Octene Copolymer Inclusion on the Morphology and Mechanical Properties of Polyamide/Polpropylene Blends", *Journal of Reinforced Plastics and Composites*, Vol. 25 (9), 933-955.
32. Chow W S, Mohd Ishak Z A, Karger-Kocsis J, Apostolov A A and Ishiaku U S (2003), "Compatibilizing Effect of Maleated Polypropylene on the Mechanical Properties and Morphology of Injection Molded Polyamide 6/ Polypropylene/ Organoclay Nanocomposites", *Polymer*, Vol. 44 (24), 7427-7440.
33. Karasek K R, Goretta K C, Helberg D A and Routbort J L (1992), "Erosion in Bismaleimide Polymers and Bismaleimide-Polymer Composites", *Journal of Materials Science Letters*, Vol. 11, 1143–1144.